FACTA UNIVERSITATIS
Series: **Electronics and Energetics** Vol. 36, Nº 4, December 2023, pp. 485 - 497
https://doi.org/10.2298/FUEE2304485S

Original scientific paper

ELECTRO-ACOUSTIC ANALOGIES BETWEEN THERMOELASTIC COMPONENT OF THE PHOTOACOUSTIC SIGNAL AND LOW-PASS RC FILTER

Neda Lj. Stanojevic[1], Dragana K. Markushev[2], Sanja M. Aleksic[1], Dragan S. Pantic[1], Dragan V. Lukic[2], Marica N. Popovic[2], Dragan D. Markushev[2]

[1]Faculty of Electronic Engineering, University of Niš, Niš, Serbia
[2]Institute of Physics, University of Belgrade, Belgrade-Zemun, Serbia

Abstract. *This paper presents a new approach to the thermal characterization of aluminum, based on the electro-acoustic analogy between the thermoelastic component of the photoacoustic signal and the passive RC low-pass filter. The analogies were used to calculate the characteristic thermoelastic cut-off frequencies of the photoacoustic component and obtain their relationship with the thickness of the aluminum samples. Detailed numerical analysis showed that the required relationship is linear in the log-log scale and can serve as a reference curve for the given material. The results of the numerical analysis were also confirmed experimentally.*

Key words: *electro-acoustic, thermoelastic component, photoacoustic signal, RC filter*

1. INTRODUCTION

Photoacoustics, as one of the very sensitive detection methods within photothermal sciences, is based on the photoacoustic effect [1,2]. The photoacoustic effect is the effect of the formation of sound waves after the interaction of light and the matter of the periodically illuminated sample in any aggregate state. In this article, we will deal with the analysis of solid samples. The sound generated in solids after light-matter interaction is usually called a photoacoustic signal. It is a complex combination of at least two components: thermo-diffusion and thermoelastic [3,4]. If a plate-shaped solid sample is illuminated by a modulated light source from one side, the thermo-diffusion component is generated by the periodic expansion and contraction of a thin layer of air adjacent to the unilluminated surface of the sample. On the other hand, periodic bending of the same sample occurs because of different temperatures at illuminated and nonilluminated sample surfaces. Such bending causes the

Received February 13, 2023; revised April 10, 2023; accepted May 03, 2023
Corresponding author: Neda Stanojevic
Faculty of Electronic Engineering, University of Niš, Aleksandra Medvedeva 14, 18000 Niš, Serbia
E-mail: neda.stanojevic@elfak.ni.ac.rs

compression of the gas in the sample vicinity, changing gas pressure, and thus the thermoelastic component is generated [5,6]. Both components bring physical characteristics of the illuminated sample material, usually given in the terms of different coefficients: thermal diffusion, D_T, thermal conduction k, linear thermal expansion α_T, etc.

The thermoelastic component of the photoacoustic signal is specific in that its frequency response, both amplitude, and phase, is very similar to the frequency response of a low-pass RC filter [7-10]. Therefore, in this paper, we will try to establish an electro-acoustic analogy between the thermoelastic response and the response of a passive RC low-pass filter. We will show that the amplitude and phase graphs of the thermoelastic component can be understood as Bode plots and analyzed with the same transfer function as the aforementioned RC filter. Also, we will show that characteristic cut-off frequencies obtained from such an analysis can be used to obtain the thermal diffusion coefficient of the material from which the examined sample is made.

2. THEORETICAL BACKGROUND

2.1. Theory of thermoelastic bending

A typical photoacoustic setup for material characterization (an open-cell setup) involves illuminating the sample with a modulated light source intensity (pure sinusoid I, Fig.1, with frequency $\omega=2\pi f$, f is the modulation frequency) [5,11-13]. The sample is surrounded by air and placed on top of the microphone. Illumination leads to a change in the thermal state of the sample, which results in different temperatures on its illuminated and non-illuminated sides. Different temperatures cause the sample to bend (see Fig.1). The bending is periodic and elastic, following the rhythm of the light source modulation. The bending of the sample described in this way is called thermoelastic bending. Theory of thermoelastic bending [14,15] derived equations describing the thermoelastic bending of a uniform-thickness plate being heated.

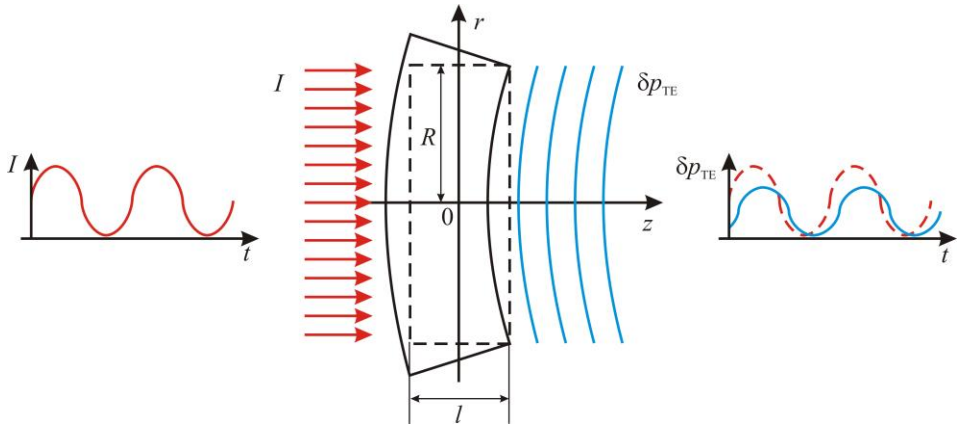

Fig. 1 The basic scheme of the open-cell setup shows the thermoelastic bending of a periodically illuminated sample of thickness l, radius R, and the thermoelastic sound component δp_{TE} generation and propagation along the z - axis (axis of heat propagation)

Thermoelastic bending produces a back-side acoustic wave, so-called thermoelastic component of the photoacoustic signal δp_{TE} (pure sinusoid, same frequency as I, different amplitude and phase), with a pressure detected by the microphone membrane defined as [16,17]:

$$\delta p_{\mathrm{TE}} = \alpha_T \frac{\gamma p_0}{V_0} \frac{3\pi R^4}{l^3} M_T \,, \tag{1}$$

where α_T is the coefficient of linear thermal expansion, γ, p_0 and V_0 are the adiabatic constant, pressure and volume of the air in microphone, respectively, and M_T is the first moment of the plate temperature change along the z - axis, defined as [15-17]:

$$M_T = \int_{-l/2}^{l/2} z T_s(z,\omega)\,\mathrm{d}z \,. \tag{2}$$

Here $T_s(z,\omega)$ is the temperature distribution along the z - axis. When M_T is calculated in the case of a surface absorber, it can be written as [15-17]:

$$M_T = \frac{I_0}{k\sigma_i^3} \cdot \left[\tanh\left(\frac{\sigma_i l}{2}\right) - \frac{\sigma_i l}{2} \right], \tag{3}$$

where I_0 is the amplitude of excitation, k is the thermal conductivity of the sample material, and $\sigma_i = (1+j)\sqrt{\omega / 2D_T}$ is the complex thermal diffusion coefficient (j is the imaginary unit, D_T is the diffusion coefficient).

Being the complex number, δp_{TE} has an amplitude A_{TE} and a phase φ_{TE} (see Appendix I). Usually, their common modulation frequency f response plots are presented as in Fig. 2.a (A_{TE}) and Fig. 2.b (φ_{TE}), where calculations are performed for the pure aluminum circular plate sample having the thickness, $l = 100\ \mu m$, and a radius, $R = 2.5\ mm$, with basic thermal properties given in Table I [17,18].

Table 1 Aluminum sample parameters used in Eq. (1-3)

Thermal conductivity, k / (W/mK)	237
Heat capacity, C / (J/kgK)	900
Density, ρ / (kg/m^3)	2700
Heat diffusion D_T / (10^{-5} m^2/s)	9.75
Linear thermal expansion, α_T / (10^{-6} 1/K)	23.1

Since δp_{TE} represent sound, the A_{TE} values can also be represented in decibels (dB), Figure 2a (A_{dB}), using the equation:

$$A_{\mathrm{dB}} = 20 \log \frac{A_{\mathrm{TE}}}{A_{\mathrm{TE}}^{\max}} \,, \tag{4}$$

where A_{TE}^{max} is the maximal amplitude value in the given frequency domain. Corresponding phase φ values are represented in Figure 5b. Both quantities, A_{dB} and φ, have the same shape in the frequency domain as A_{TE} and φ_{TE}, but different numerical values.

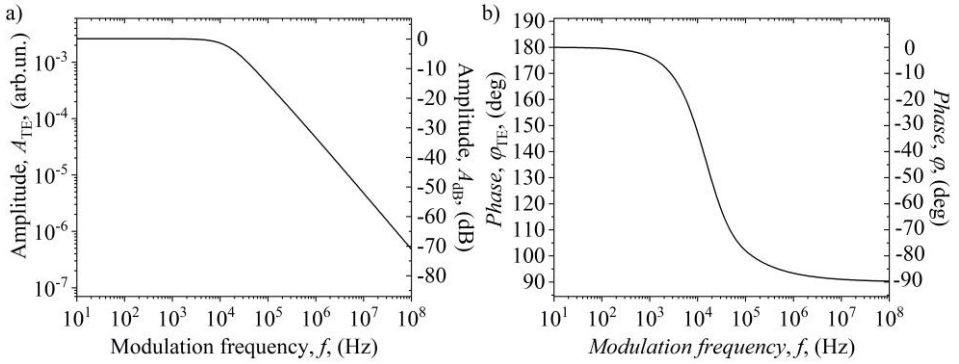

Fig. 2 a) Amplitudes A_{TE} and b) phases φ_{TE} of the photoacoustic signal thermoelastic component δp_{TE} (Eq. (1)) as a function of the modulation frequency f. Amplitude A_{dB} in decibels (Eq.(4)) and corresponding phase φ values were depicted, also

2.2. Low-pass RC filter

Analyzing δp_{TE} response from Figure 2, one can see that our photoacoustic system can pass certain frequencies while attenuating others. In other words, our system acts as a filter, so the analogy can be made with a passive low-pass RC filter, presented in Figure 3 in (a) time and (b) frequency domain [7-10]. Here, U_{in} is an input voltage, U_{out} is an output voltage (voltage across the capacitor), $Z_R = Z$ is the resistor impedance, and $Z_C = 1/sC$ is the capacitor impedance, where s is a complex number $s = \sigma + j\omega$ (j is the imaginary unit, σ is the exponential decay constant, and ω is the sinusoidal angular frequency).

By viewing the circuit (Figure 3b) as a voltage divider, and considering a special case of sinusoidal steady state in which the input (red line) and output (blue line) voltage consists of a pure sinusoid (no exponential decay, $\sigma = 0$, $s = j\omega$), the transfer function $H(j\omega)$ from the input voltage to the voltage across the capacitor can be given in the form [7-10]:

$$H(j\omega) = \frac{U_{out}(j\omega)}{U_{in}(j\omega)} = \frac{1}{1 + j\omega RC} = \frac{1}{1 + j\dfrac{\omega}{\omega_0}} \tag{5}$$

assuming zero initial conditions, where $\omega_0 = 1/RC$ is the cut-off frequency, a boundary frequency at which energy flowing through the circuit begins to be attenuated. As a complex number, $H(j\omega)$ has an amplitude $|H(j\omega)|$ and the phase φ which can be presented in the forms:

$$\left|H(j\omega)\right| = \frac{1}{\sqrt{1 + \left(\dfrac{\omega}{\omega_0}\right)^2}} \tag{6}$$

and

$$\varphi = -\arctan\left(\frac{\omega}{\omega_0}\right) \tag{7}$$

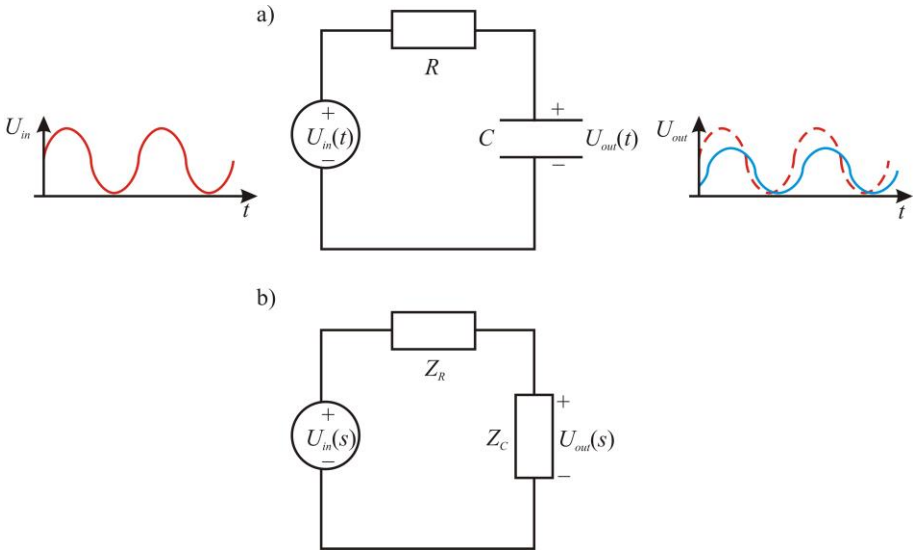

Fig. 3 A simple scheme of RC low - pass filter in a) time and b) frequency domain.

Usually, the magnitude A is calculated in decibels (dB) using [7-10]:

$$A = 20\log\left|H\left(j\omega\right)\right| \tag{8}$$

The standard representations of a given low-pass RC filter A and φ are Bode plots [19,20] (Figure 4), obtained using Eq.(6-8), taking into account that $\omega_0 = 2\pi f_0$, and $f_0 = 1.5 \cdot 10^4\ s^{-1}$.

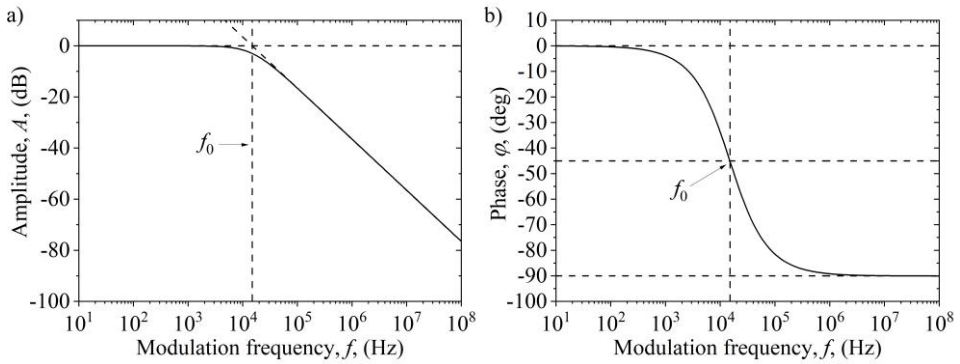

Fig. 4 Bode a) amplitude A and b) phase φ plots of the RC low-pass filter response in frequency domain. Dashed auxiliary lines define the position of f_0

3. RESULTS AND DISCUSSION

3.1. Theoretical procedure

Based on the introductory remarks, both the photoacoustic system (Figure 1) and the low - pass RC filter (Figure 3) can be considered as the linear time - invariant (*LTI*) systems [21,22] whose frequency responses after sinusoidal inputs (excitations) are shown in Figures 2 and 4. The cut - off frequency f_{TE} of the thermoelastic component can be found, using the Bode diagrams from Figure 2 for $l = 100\,\mu m$ and $R = 2.5\,mm$ values, in two ways: 1) approximately, finding the intersection of the amplitude asymptotes (dashed lines in Figure 5a), and/or 2) explicitly, by fitting the amplitude (Figure 5.a) with a function y_{TE}, based on Eqs. (6) and (8), given in the form:

$$y_{\mathrm{TE}} = 20\log\left(\left(1+\left(\frac{x}{m}\right)^2\right)^{-\frac{n}{2}}\right) \tag{9}$$

where, $x = f$ is the modulation frequency, and m and n are fitting parameters, $f_{TE} = m$ and the slope is $n/2$. This expression is commonly used in electronics to describe the cascade connection of the RC filters, but in our case, it is intended to cover a slope, different to the RC filter. The results of the δp_{TE} amplitude fitting procedure (Figure 5a, blue line) are as follows: $f_{TE} = (15660 \pm 60)$ and $n = (9786 \pm 6)\cdot 10^{-4}$. The value of f_{TE} is depicted in Figures 5.a.b, using dashed vertical line.

Applying the obtained f_{TE} value in A (Eq. (8)) and φ (Eq. (7)) one can calculate corresponding low - frequency bandpass RC filter responses (red lines in Figure 5.a, and Figure 5.b, respectively). Obvious discrepancies between blue and red lines can be observed at higher frequencies for both amplitudes and phases. This result is only a consequence of the fact that real systems (photoacoustics) are not the ideal analogies (RC filters).

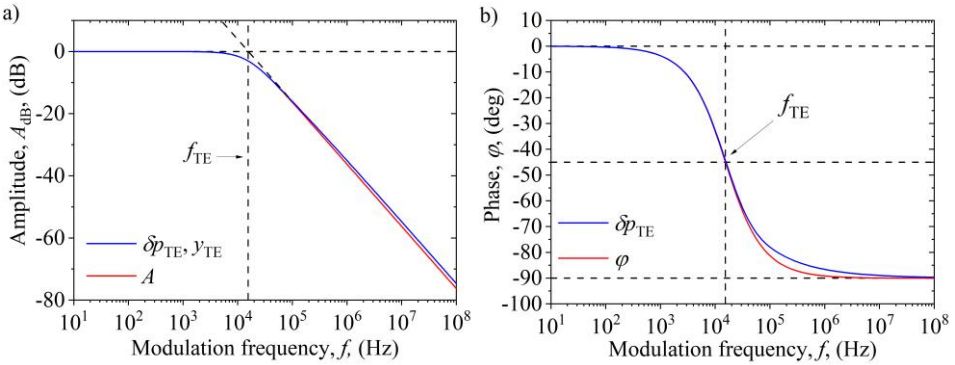

Fig. 5 Bode a) amplitude and b) phase plots of the photoacoustic signal thermoelastic component δp_{TE} obtained theoretically (Eq. (1)) in the case of aluminum circular plate having the thickness l and radius R, with basic thermal parameters which are given in Table I. Cut-off frequency f_{TE} is obtained using y_{TE} fit (Eq. (9)). Red line A is obtained using Eq. (8) and f_{TE}

Using the same procedure, we can fit thermoelastic components for aluminum samples of the same shape but different thicknesses: from l_{min} = 10 to 100 μm in steps of 10 μm, and from 100 to l_{max} = 1000 μm in steps of 100 μm (Figure 6). All presented thermoelastic components of the photoacoustic signals are obtained using Eq. (4) and sample parameters are given in Table 1.

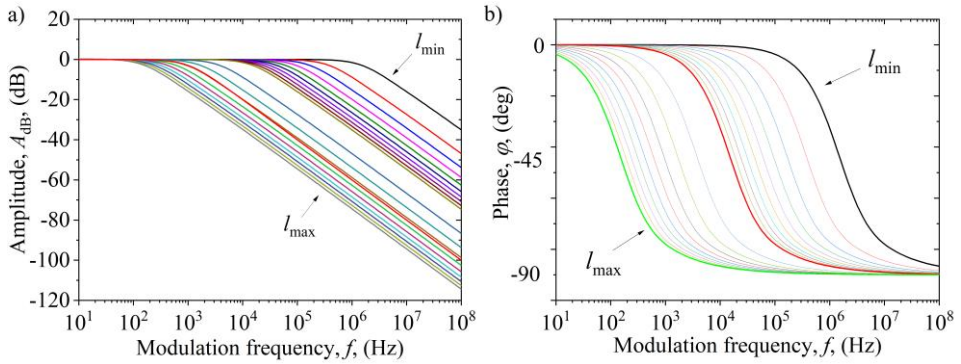

Fig. 6 Bode a) amplitude and b) phase plots of the photoacoustic signal thermoelastic component δp_{TE} obtained theoretically (Eq. (1)) in the case of aluminum circular plate with different thicknesses l and constant radius R, with basic thermal parameters which are given in Table 1

The fitting results obtained by Eq. (9) are shown in Table II, based on which the dependence of f_{TE} on the sample thickness l is drawn (red line, Figure 7).

Table 2 Fitting results of an aluminum sample estimation of cut - off frequency as a function of sample thickness.

Sample thickness l / ($\times 10^{-6}$ m)	Cut-off frequency f_{TE} / (Hz)
10	1480460
20	376097
30	168860
40	95666.5
50	61560.5
60	42936.7
70	31658.7
80	24313.1
90	19261.3
100	15638.0
200	3965.95
300	1776.11
400	1004.17
500	645.126
600	449.404
700	331.063
800	256.923
900	204.806
1000	167.771

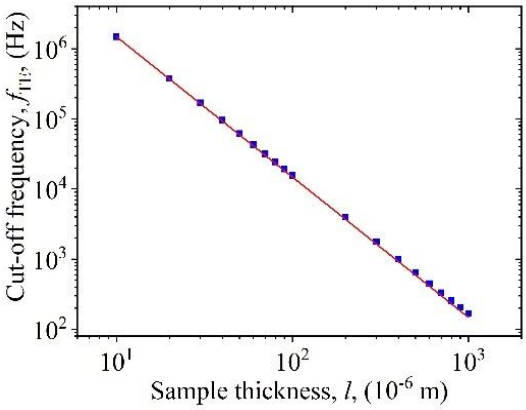

Fig. 7 Log-log scale of f_{TE} dependence on sample thickness l. Red line represent the fit line obtained using Eq. (11)

Mathematically, the dependence of f_{TE} on l in a logarithmic scale (Figure 7) can be obtained by finding the value of $\sigma_i\, l/2$ in the square bracket of Eq. (3), in the case of $f=f_{TE}$, using:

$$\frac{|\sigma_i| l}{2} = b \tag{10}$$

or

$$f_{\mathrm{TE}} = \frac{2}{\pi} \cdot \frac{D_T}{l^2} \cdot b^2 \tag{11}$$

considering that $|\sigma_i| = \sqrt{\omega / D_T}$, and $\omega = \omega_{\mathrm{TE}} = 2\pi f_{\mathrm{TE}}$. Fitting the data from Figure 7 with Eq. (11) (red line), it is obtained that $b = 1.545$. Obtained data fit line represents the reference value of the aluminum samples considered as surface absorbers. It can be used to check the validity of measurements and deviations from theoretical model and/or literature values due to various sample impurities, physical damages, etc.

3.2. Experimental validation

To validate the suggested δp_{TE} analysis procedure based on electro-acoustic analogy with low - pass RC filter and Eq.(11), we measured and analyzed the photoacoustic response of aluminum sample in 20 Hz – 20 kHz modulation frequency f domain, using a typical open-cell photoacoustic experimental set-up (see Appendix II). The investigated sample was circular in shape, having a thickness, $l = 155\ \mu m$, and a radius, $R = 2.5\ mm$. The results of such analysis are shown in Figures 8 - 11. Using the well-known method of the signal "cleaning" from the instrumental influence [23-25], we obtained the "real" signal δp (blue line, Figure 8) from the measured experimental values S_{exp} (Figure 8, asterisks), within the experimental error of 5 %.

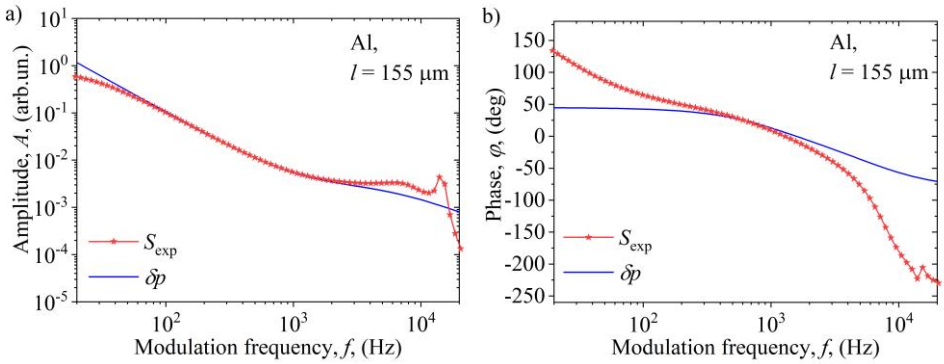

Fig. 8 a) Amplitude and b) phase of the aluminum A_1 sample experimental signal S_{exp} (asterisks) and the "real" signal δp (blue line), signal freed from the instrumental influences

Applying the composite piston model on the "real" signal δp [4,16,17], both components were obtained: thermo-diffusion, δp_{TD}, and thermoelastic, δp_{TE}, (Figure 9, green and red lines, respectively). One must take into account that model suggest simple relationship: $\delta p = \delta p_{\mathrm{TD}} + \delta p_{\mathrm{TE}}$. Obtained frequency response of these components correspond to the thermal characteristics of the investigated sample given in Table I.

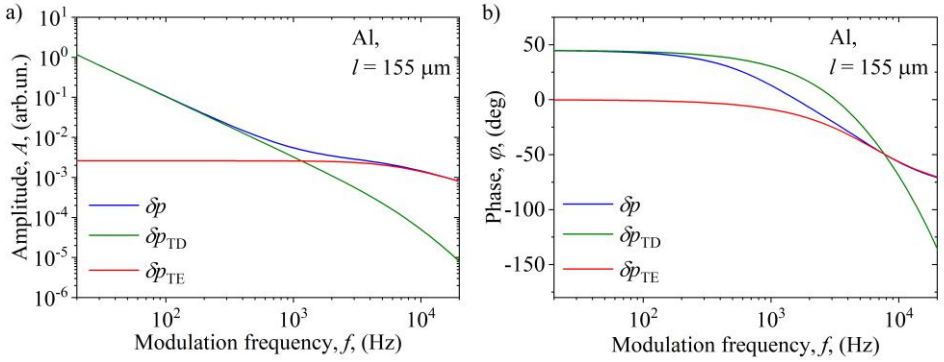

Fig. 9 a) Amplitude and b) phase of the "real" δp signal and its components (thermo-diffusion, δp_{TD}, and thermoelastic, δp_{TE}), obtained using the composite piston model [4,16,17]

Analyzing obtained thermoelastic component with Eq. (12) (Figure 10), the value $f_{TE155} = (6275 \pm 325)$ *Hz* is obtained for the measured sample.

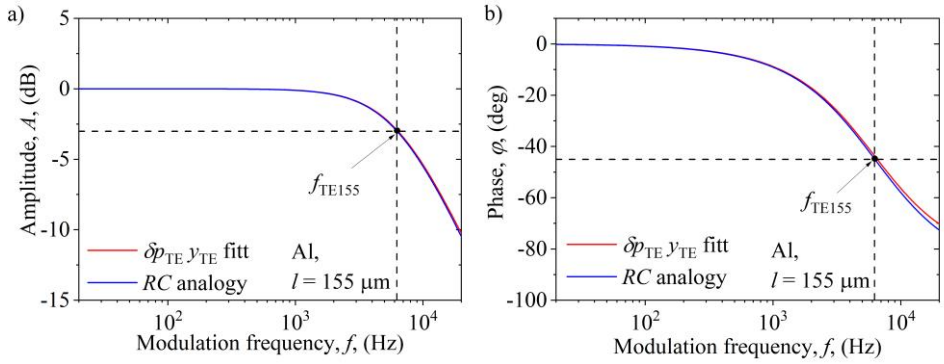

Fig. 10 Analysis of a) amplitude A and b) phase φ of δp_{TE} using Eq. (9) (red line) and the analogue curve of the RC low - pass filter obtained by equations (7) and (8) and frequency $f_0 = f_{TE155}$

The value of f_{TE155} is plotted on the dependence graph $f_{TE} = f(l)$ (Figure 11, blue line) copied from Figure 7 (red line). It is obvious from Figure 11 that the full matching of f_{TE155} with the blue line confirms the correctness of Eq. (11).

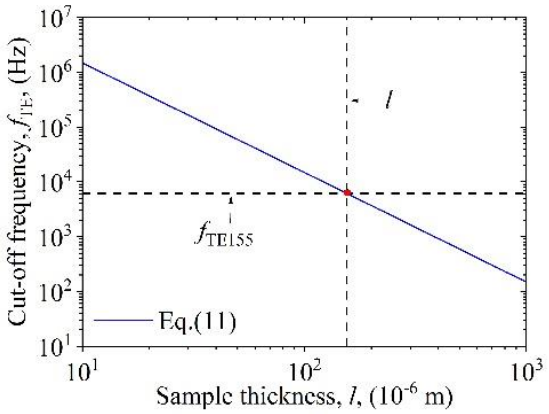

Fig. 11 Dependence of the characteristic thermoelastic cut-off frequency, f_{TE}, on the thickness of the sample, l, with the value of f_{TE155} (red circle) of the experimental *Al* sample having a thickness of 155 microns

4. CONCLUSIONS

In this paper, we have shown that it is possible to make an analogy between the response of the thermoelastic component of the photoacoustic signal in the frequency domain and the frequency response of the low - pass RC filter because both systems behave as linear time - invariant systems. It was established that the thermoelastic component could be numerically processed by a function created based on of the RC filter transfer function. As a result of such processing, the characteristic cut - off

frequency f_{TE} of the thermoelastic component is obtained, the value of which changes by changing the thickness of the tested sample. It was observed that the dependence of f_{TE} on sample thickness l in a logarithmic scale is linear, and that f is proportional to $1/l^2$. The proportionality coefficient contains the value of the thermal diffusion coefficient D_T and the numerical value of the constant b that defines the value of temperature moment M_T in the case when $f = f_{TE}$. Since both D_T and b constants are related to the tested sample, the dependence $f_{TE} \sim 1/l^2$ can be used to define a reference curve for the thermal characterization of the sample material. To confirm the slope of the reference curve, the photoacoustic response of a 155 μm thick aluminum sample was measured with the open-cell experimental set-up, and its thermoelastic component was processed. The obtained value of f_{TE} entirely coincides with the established reference curve of aluminum obtained by theoretical analysis, thus confirming the correctness of the newly established methodology for the thermal characterization of the material.

The importance of the presented article is that it can serve as a basis for the future application of electro-acoustic analogies in the description of transport processes both in physics and electronics [26] (for example, characterization of semiconductors through the contribution of excess carriers) and in medical sciences [27,28] (transport and exchange of energy by diffusion, the transmission of information by the nervous system, modelling axons as electrical cables, forming axon circuits, etc.).

Acknowledgement: *This work has been supported by the Ministry of Education, Science and Technological Development of the Republic of Serbia and by the Institute of Physics Belgrade, through the grant by the Ministry of Science, Technological Development and Innovations of the Republic of Serbia.*

REFERENCES

[1] D. Almond and P. Patel, *Photothermal Science and Techniques*, Chapman & Hall, London, 1996.
[2] S. E. Bialkowski, N. G. C. Astrath, M. A. Proskurnin, *Photothermal Spectroscopy Methods for Chemical Analysis*, 2nd Edition, New York: John Wiley, 2019.
[3] A. Rosencwaig and A. Gersho, "Theory of the photoacoustic effect with solids", *J. Appl. Phys.*, vol. 47, p. 64-69, 1976.
[4] F. McDonald and G. Wetsel, "Generalized theory of the photoacoustic effect", *J. Appl. Phys.*, vol. 49, pp. 2313-2322, 1978.
[5] L. F. Perondi and L. C. M. Miranda, "Minimal-volume photoacoustic cell measurement of thermal diffusivity: Effect of the thermoelastic sample bending", *J. Appl. Phys*, vol. 62, no. 7, pp. 2955-2959, 1987.
[6] A. L. Glazov and K. L. Muratikov, "Generalized thermoelastic effect in real metals and its application for describing photoacoustic experiments with al membranes", *J. Appl. Phys.*, vol. 128, no. 9, p. 095106, 2020.
[7] L. D. Paarman, *Design and analysis of analog filters*, Kluwer Academic Publishers, USA, 2001.
[8] L. E. Frenzel Jr., *Principals of Electronic Communications Systems*, Fourth Edition, McGraw-Hill, 2016.
[9] C. K. Alexander, M. N. O. Sadiku, *Fundamentals of electric circuits*, McGraw-Hill Education, USA, 2017.
[10] Okawa Electric Design (2019), *RC Low-pass Filter Design Tool*. Available at: http://sim.okawa-denshi.jp/en/CRlowkeisan.htm
[11] A. Somer, F. Camilotti, G. Costa, C. Bonardi, A. Novatski, A. Andrade, V. Kozlowski Jr and G. Cruz, "The thermoelastic bending and thermal diffusion processes influence on photoacoustic signal generation using open photoacoustic cell technique", *J. Appl. Phys.*, vol. 114, no. 6, p. 063503, 2013.
[12] A. Somer, A. Gon¸calves, T. V. Moreno, G. K. da Cruz, M. L. Baesso, N. G. C. Astrath and A. Novatski, "Photoacoustic signal with two heating sources: theoretical predictions and experimental results for the open photoacoustic cell technique", *Meas. Sci. Technol.*, vol. 31, no. 7, p. 075202, 2020.

[13] J. A. Balderas-Lopez and A. Mandelis, "Thermal diffusivity measurements in the photoacoustic open-cell configuration using simple signal normalization techniques", *J. Appl. Phys.*, vol. 90, no. 5, pp. 2273-2279, 2001.
[14] B. A. Boley and J. H. Weiner, *Theory of Thermal Stresses*, Wiley, New York, 1960.
[15] G. Roussett, F. Lepoutre and L. Bertrand, "Influence of thermoelastic bending on photoacoustic experiments related to measurements of thermal diffusivity of metals", *J. Appl. Phys.*, vol. 54, pp. 2383-2391, 1983.
[16] D. D. Markushev, J. Ordonez-Miranda, M. D. Rabasovic, M. Chirtoc, D. M. Todorovic, S. E. Bialkowski, D. Korte and M. Franko, "Thermal and elastic characterization of glassy carbon thin films by photoacoustic measurements", *The European Phys. J. Plus*, vol. 132, no. 33, pp. 1-9, 2017.
[17] D. D. Markushev, J. Ordonez-Miranda, M. D. Rabasović, S. Galović, D. M. Todorović and S. E. Bialkowski, "Effect of the absorption coefficient of aluminium plates on their thermoelastic bending in photoacoustic experiments", *J. Appl. Phys.*, vol. 117, p. 245309, 2015.
[18] J. R de Laeter, et al, "Atomic weights of the elements: Review 2000", *Pure Appl. Chem.*, vol. 75, pp. 683-800, 2003.
[19] W. M C. Sansen, *Analog design essentials.* Dordrecht, The Netherlands: Springer. pp. 157-163.
[20] R. K. Rao Yarlagadda, *Analog and Digital Signals and Systems*. Springer Science & Business Media. 2010, p. 243.
[21] C. L. Phillips, J. M. Parr and E. A. Riskin, *Signals, systems and Transforms.* Prentice Hall. 2007.
[22] J. P. Hespanha, *Linear System Theory*. Princeton University Press, 2009.
[23] D. D. Markushev, M. D. Rabasović, D. M. Todorović, S. Galović and S. E. Bialkowski, "Photoacoustic signal and noise analysis for Si thin plate: Signal correction in frequency domain", *Rev. Sci. Instrum.*, vol. 86, p. 035110, 2015.
[24] M. N. Popovic, M. V. Nesic, S. Ciric-Kostic, M. Zivanov, D. D. Markushev, M. D. Rabasovic, S. P. Galovic, "Helmholtz Resonances in Photoacoustic Experiment with Laser-Sintered Polyamide Including Thermal Memory of Samples", *Int. J. Thermophys.*, vol. 37, p. 116, 2016.
[25] S. M. Aleksić, D. K. Markushev, D. S. Pantić, M. D. Rabasović, D. D. Markushev and D. M. Todorović, "Electro-acoustic influence of measuring system on the photoacoustic signal amplitude and phase in frequency domain", *FU Phys Chem Tech*, vol. 14, no. 1, pp. 9-20, 2016.
[26] S. Galovic, Z. Soskic and M. Popovic, "Analysis of photothermal response of thin solid films by analogy with passive linear electric networks", *Thermal Sci.*, vol. 13, no. 4, pp. 129-142, 2009.
[27] R. Deaton, M. Garzon and R. Yasmin, "Systems of axon-like circuits for self-assembled and self-controlled growth of bioelectric networks", *Sci. Reports*, vol. 12, p. 13371, 2022.
[28] P. Alcami and A. El Hady, "*Axonal Computations*", *Front. Cell. Neurosci.*, vol. 13, p. 413, 2019.

APPENDIX I

Considering Eqs (1-3) the expression for δp_{TE} can be written in the form

$$\delta p_{TE} = \alpha_T \frac{\gamma I_0 p_0}{2V_0 k} \frac{3\pi R^4}{(\sigma_i l)^2} \cdot \left[\frac{\tanh\left(\frac{\sigma_i l}{2}\right)}{\frac{\sigma_i l}{2}} - 1 \right], \tag{12}$$

as a complex number δp_{TE} has its amplitude and phase, whose analytical expressions are complicated. But, for electro-acoustic analogies [26], with the series expansion of the expression in square brackets, one can obtain a simplified expression for δp_{TE} of the form

$$\delta p_{TE} = -3\pi\alpha_T \frac{\gamma I_0 p_0 R^4}{16 V_0 k} \cdot \left[\frac{1}{1 + j\frac{\omega}{\omega_{TE}}} \right], \tag{13}$$

whose amplitudes and phases are given as

$$A_{TE}(j\omega) = \left|\delta p_{TE}(j\omega)\right| \sim \frac{1}{\sqrt{1+(\omega/\omega_{TE})^2}}, \text{ and } \varphi = -\arctan\left(\frac{\omega}{\omega_{TE}}\right). \qquad (14)$$

Here $\omega_{\mathrm{TE}} = D_T / (l/2b)^2$, and $\sqrt{2} \le b < \sqrt{6}$, depending on number of terms in series expansion.

APPENDIX II. EXPERIMENTAL SET-UP

The experimental setup of the open-cell used in this work is presented in Figure 12. It is a homemade non-commercial setup, explained in detail somewhere else [23,24]. As a light source, a red laser diode with a wavelength of 650 nm, modulated by a frequency generator from the control unit, was used. The photodiode controls the operation of the laser diode and its signal is recorded by the signal processing unit. As a sample, a thin circular aluminum plate, 3 mm in diameter and 155 microns thick, was used, and placed on the microphone's opening. The sample and the microphone together form the so-called photoacoustic cell of minimal volume.

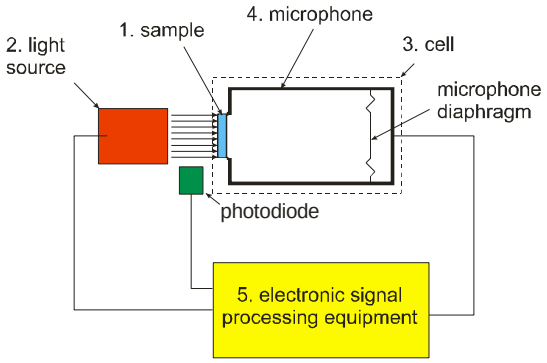

Fig. 12 Simple scheme of the open-cell photoacoustics experimental setup used in our measurements.

The sound created by the illumination of the sample spreads through the air in the cell to the microphone membrane, which records it as a photoacoustic signal, converts it into a voltage signal and forwards it to the signal processing unit for further processing. The PC is used simultaneously as a control (frequency generator) and a signal processing unit. (lock-in amplifier). As a replacement for the instrument, the computer's sound card emulates the lock-in amplifier's operation, with which we record the amplitude and phase of the measured signal (the signal from the photodiode is used as a reference signal).